The **suspended sediment load** in the North Caucasus mountains primarily **decreased** at an average rate of **–1.2% per year** throughout the entire XXth century. After **1988–1994**, the rate increased significantly to –12%.

Insights into spatial and temporal changes in suspended sediment yield in the Caucasus Mountains during the Anthropocene

Anatolii Tsyplenkov [1,2] tsyplenkova@landcareresearch.co.nz
Valentin Golosov [2,3,4]

[1] Manaaki Whenua Landcare Research, Palmerston North, New Zealand
[2] Lomonosov Moscow State University, Faculty of Geography, Moscow, Russia
[3] Institute of Geography of the Russian Academy of Sciences, Laboratory of Geomorphology, Moscow, Russia
[4] Kazan Federal University, Kazan, Russia

Regional suspended sediment yield dynamics

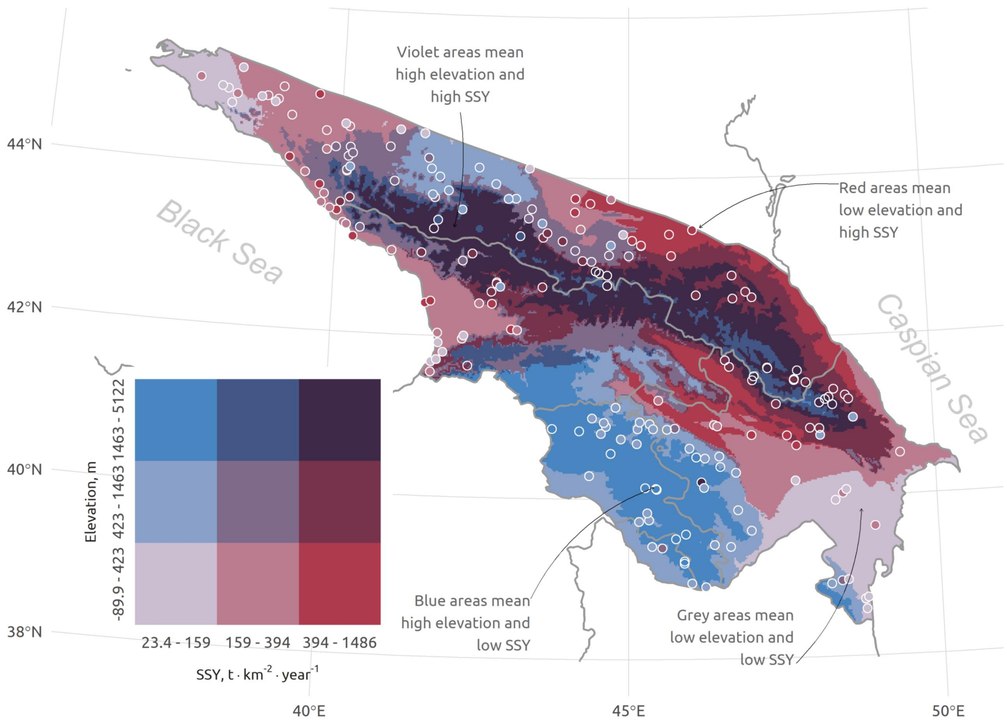

Figure 1. Spatial patterns of estimated SSY for the Caucasus Region based on mean interannual values

1) We presented the largest SSY ($t \cdot km^{-2} \cdot year^{-1}$) database to date for the Caucasus region. By analysing measured mean interannual SSY values from **244** pristine catchments, we discovered that the SSY values in the Caucasus are comparable in range and average to those found in catchments within European alpine climatic zones (i.e. 426 ± 71.9 $t \cdot km^{-2} \cdot year^{-1}$).

2) Despite the potential for significant uncertainties in the SSY values, our analysis revealed clear spatial patterns of SSY distribution across the Caucasus region (see *Fig. 1*).

3) Partial correlation analyses (PLSR) have demonstrated that topographical proxies, such as height above the nearest drainage ($HAND$) and the normalized steepness index (K_{sn}), are among the most significant factors controlling SSY.

How did suspended sediment load change during the Anthropocene?

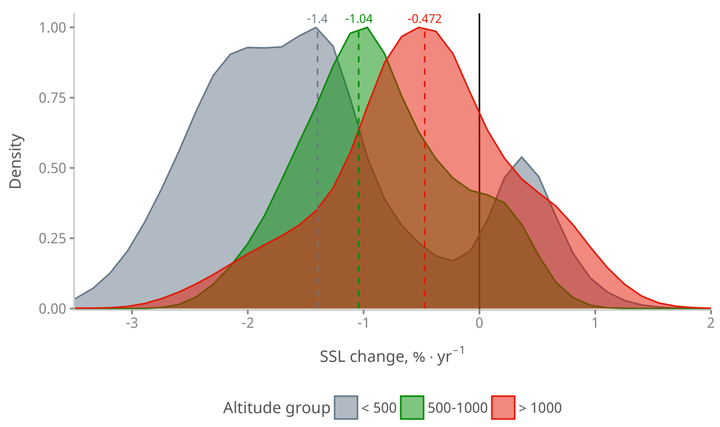

Figure 2. Density plots of trend magnitudes for SSL ($\% \cdot year^{-1}$)

4) Closer look at the North Caucasus using **33 unregulated gauging stations** in the Terek River basin, allowed us to examine the temporal changes in suspended sediment load (SSL, $t \cdot year^{-1}$) throughout the 1925-2018 period.

5) In general, the SSL over the last century has changed relatively synchronously across most rivers in the Terek basin (see *Fig. 2*).

6) At all gauges, when grouped by altitude, the mode values of SSL trends increase with altitude. This indicates that the decline in SSL is more pronounced in basins at lower altitudes than in those at higher altitudes. This serves as evidence that gauging stations at higher elevations are less susceptible to significant reductions in suspended sediment load.

When and why did these changes happen?

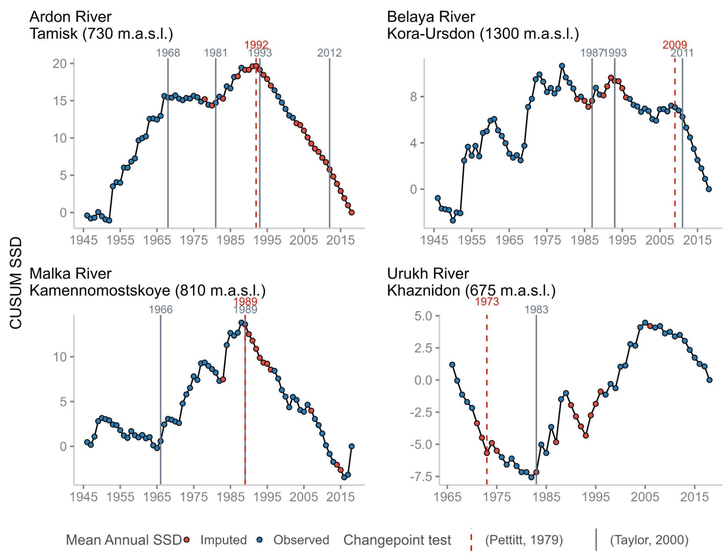

Figure 3. Cumulative sum (CUSUM) charts for the mean annual SSD

7) The CUSUM charts analysis revealed a change point roughly within the same range of years at various gauging stations (see example at *Fig 3.*). As a result, several transition years are expected in the North Caucasus: **increasing trends from the 1950s and decreasing trends from 1988-1994.**

8) The latter is most likely due to a decrease in glacier areas and a decrease in the area of arable land. It is critical for catchments with a high cropland fraction in the foothill belt (<500 m.a.s.l.). At the same time, an absence of a pronounced trend or even an insignificant increase in suspended sediment flux was established for some river basins.

9) In addition, we found that the share of the glacierized area has a strong positive impact on SSL trends (Spearman ρ = 0.73, p < 0.0001). This indicates that SSL of more glacierized catchments is likely to decrease slower (*Fig. 4b*).

10) On the other hand, SSL change is also larger in catchments with large forest cover (cf. *Fig. 4d*), that is, more pristine conditions.

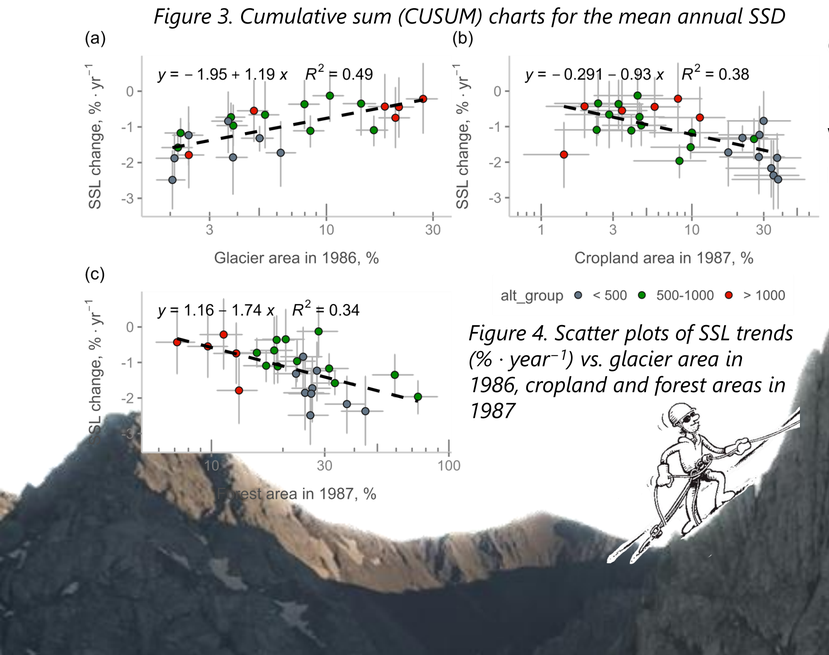

Figure 4. Scatter plots of SSL trends ($\% \cdot year^{-1}$) vs. glacier area in 1986, cropland and forest areas in 1987

Additional information

Suspended Sediment Yield (SSY) and Load (SSL)

$$SSY = \frac{\sum \frac{\bar{Q} \cdot \overline{SSC} \cdot 31.5 \cdot 10^3}{A}}{n}$$

where SSY is the mean annual suspended sediment yield, $t \cdot km^{-2}$ $year^{-1}$; Q is the mean annual water discharge, $m^3 \cdot s^{-1}$; SSC is the mean annual suspended sediment concentration, $g \cdot m^{-3}$; A is the catchment area, km^2; n is the measuring period length in years.

$$SSL = 31.5 \cdot 10^3 \cdot \overline{SSD} = 31.5 \cdot 10^3 \cdot \bar{Q} \cdot \overline{SSC}$$

where SSL is the mean annual suspended sediment load, $t \cdot year^{-1}$; SSD is the mean annual suspended sediment discharge, $kg \cdot sec^{-1}$.

Uncertainties and Limitations

We considered two main sources of SSL measuring errors and using Monte-Carlo simulations estimated 95% credible intervals. In the equation below, U_{ME} reflected the correction associated with measuring errors, U_{FF} represented the correction associated with the unmeasured finer fraction.

$$SSL_{cor} = SSL \cdot \frac{U_{ME}}{1 - U_{FF}}$$

U_{ME} reflects the integrated effect of errors on individual runoff discharge measurements, suspended sediment concentration measurements, and uncertainties due to intra-daily variation in runoff and sediment concentrations not captured by the measurements. Previous studies reported that these errors are commonly 20%–30% (Harmel et al., 2006; Steegen & Govers, 2001; Vanmaercke et al., 2015). U_{ME} was sampled from a normal distribution with mean of 1 and standard deviation of 0.30.

At Russian gauging stations, suspended sediment concentration is measured by the gravimetric method using **paper filters** with pore sizes ranging from **2 to 3 µm** (so-called «blue tape», deashed filters, «ТУ 6-09-1678-86» specification) according to Handbook for hydrological measurements at these gauging stations (РД 52.08.104-2002). However, in world practice **a membrane filter** with pore size of **0.45 µm** is typically used for SSC measurement.

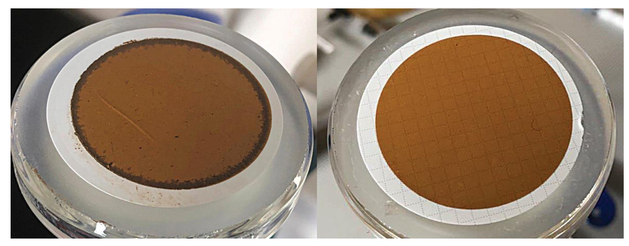

Figure A. Membrane filter with pore size of 0.45 µm (left) and paper filter with pore size of 2 µm (right). Photo by Sergey Chalov.

We performed a brief exploratory data analysis of particle size distribution from Williams and Rosgen (1989) to estimate how pore size impacts total measured suspended sediment concentration. We found that out of 216 samples, the mean percent by weight finer than 3 µm was 24.7%, with a corresponding standard deviation of 9.5%. The proportion of the finer fraction can vary from 8% to 43% (i.e., the 2.5% and 97.5% quantile) depending on the season and river. Hence, UFF was simulated as a random number from a normal distribution with a mean of 0.247 and a standard deviation equal to 0.095. Evidently, U_{FF} values were restricted to values between 0.08 and 0.43.

Equation C was used to simulate respectively 1000 alternative SSL for every year and every gauging station. From these values, we calculated 95% credible intervals (CI) on every SSL value. See example below (*Fig. B*).

These simulations were further used to estimate trend uncertainties (in $\%{\cdot}year^{-1}$) as well as SSY errors.

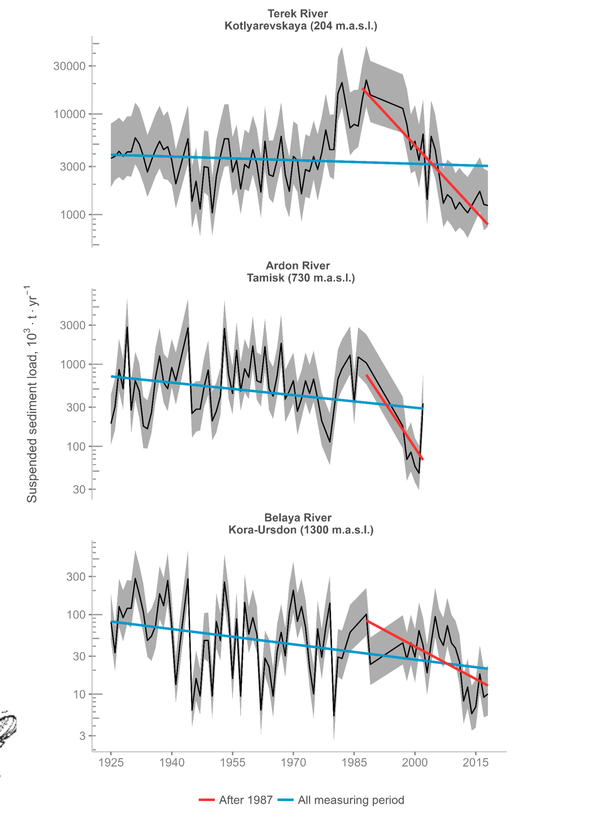

Figure B. Suspended sediment load time series for several gauging stations in the Terek basin. The black line displays the time series with the uncertainty envelope.